

# Mössbauer Spectroscopic Study of Fe<sub>2</sub>O<sub>3</sub> Nanoparticles Dispersed over a Silica Matrix

Carla Cannas, Giorgio Concas<sup>a</sup>, Anna Musinu, Giorgio Piccaluga, and Giorgio Spano<sup>a</sup>

Dipartimento di Scienze Chimiche, Università di Cagliari,  
S.P. Monserrato-Sestu km 0.700, I-09042 Monserrato (Cagliari), Italy

<sup>a</sup> Dipartimento di Fisica, Università di Cagliari and Istituto Nazionale per la Fisica della Materia,  
S.P. Monserrato-Sestu km 0.700, I-09042 Monserrato (Cagliari), Italy

Reprint requests to Dr. G. C.; Fax: +39 070 570071; E-mail: gconcas@vaxca1.unica.it

Z. Naturforsch. **54 a**, 513–518 (1999); received June 28, 1999

A series of Fe<sub>2</sub>O<sub>3</sub>-SiO<sub>2</sub> nanocomposites (9 - 33 wt% of Fe<sub>2</sub>O<sub>3</sub>) has been prepared by a sol-gel method and submitted to thermal treatments at 300 - 900 °C. The samples were characterized by X-ray diffraction and Mössbauer Spectroscopy measurements. Superparamagnetic behavior is exhibited by all the samples, indicating that the size of iron oxide grains is in the nanometer range (4 - 6 nm). Increase of iron content and temperature treatment give rise to a small particle growth, while the spread of sizes around the average value increases with the iron concentration. The Mössbauer spectra, at all the explored compositions, show a very steep increase of the peak width by treatment temperature at 900 °C, indicating the formation of the ferrimagnetic  $\gamma$ -Fe<sub>2</sub>O<sub>3</sub> phase from the antiferromagnetic amorphous Fe<sub>2</sub>O<sub>3</sub> phase, which dominates in the samples treated at lower temperatures. The samples at 28.5% and 33.2%, treated at 900 °C, also show a component of  $\gamma$ -Fe<sub>2</sub>O<sub>3</sub> in the blocked state at room temperature. Moreover, the growth of the particles favours the formation of other oxide phases ( $\alpha$  and  $\varepsilon$  phase) along with the  $\gamma$  phase.

**Key words:** Nanocomposite; Ferric Oxide; Mössbauer Spectroscopy; X-ray Diffraction.

## 1. Introduction

Recently we have reported the preparation of a series of Fe<sub>2</sub>O<sub>3</sub>-SiO<sub>2</sub> composites (9 - 33 wt% of Fe<sub>2</sub>O<sub>3</sub>) through a simple sol-gel method, that adopted Si(OC<sub>2</sub>H<sub>5</sub>)<sub>4</sub> (TEOS) and iron nitrate as precursors [1, 2]. The aim was the stabilization of  $\gamma$ -Fe<sub>2</sub>O<sub>3</sub> nanoparticles in a glass matrix, such a glass being of technological interest due to its magnetic and catalytic properties. The samples were submitted to thermal treatments in the 300 - 900 °C range and characterized through XRD, TEM, EPR and magnetic susceptibility measurements. All these techniques indicated that superparamagnetic iron (III) oxide particles with a narrow size distribution are present in such samples. However, these particles undergo a complex transformation as a function of the thermal treatments. In fact, they are mostly amorphous and antiferromagnetic in samples treated at low temperature. At  $T > 700$  °C a lot of  $\gamma$ -Fe<sub>2</sub>O<sub>3</sub> crystalline ferrimagnetic nanoparticles (4 - 6 nm) are formed, while a further increase of the temperature results in the  $\gamma$ - to  $\alpha$ -Fe<sub>2</sub>O<sub>3</sub> transformation. The variation of the iron oxide content affects the

abundance of  $\gamma$ -Fe<sub>2</sub>O<sub>3</sub> formation, which reaches the maximum percent values in the more diluted samples. In the more concentrated samples, while the amount of maghemite is still growing, antiferromagnetic  $\alpha$ -Fe<sub>2</sub>O<sub>3</sub> begins to form [2]. These results confirm the difficulty of obtaining only the  $\gamma$ -Fe<sub>2</sub>O<sub>3</sub> phase, already discussed by authors who used a similar preparation method [3, 4]. In order to improve the method, a better knowledge of the structural evolution under thermal treatment and of the different formed phases is very important. In the present paper we report a study of the above mentioned series of samples by Mössbauer spectroscopy, which is particularly effective in revealing the structural and magnetic order around iron atoms [5 -12].

## 2. Experimental

A series of iron oxide/silica composites were prepared, containing respectively 9.1, 16.9, 23.0, 28.5 and 33.2 wt% of Fe<sub>2</sub>O<sub>3</sub>. The preparation and characterization of the samples have been described in [1, 2]. The labels Fe<sub>x</sub>Y will be used in the following, where

0932-0784 / 99 / 0800-0513 \$ 06.00 © Verlag der Zeitschrift für Naturforschung, Tübingen · www.znaturforsch.com



Dieses Werk wurde im Jahr 2013 vom Verlag Zeitschrift für Naturforschung in Zusammenarbeit mit der Max-Planck-Gesellschaft zur Förderung der Wissenschaften e.V. digitalisiert und unter folgender Lizenz veröffentlicht: Creative Commons Namensnennung-Keine Bearbeitung 3.0 Deutschland Lizenz.

Zum 01.01.2015 ist eine Anpassung der Lizenzbedingungen (Entfall der Creative Commons Lizenzbedingung „Keine Bearbeitung“) beabsichtigt, um eine Nachnutzung auch im Rahmen zukünftiger wissenschaftlicher Nutzungsformen zu ermöglichen.

This work has been digitalized and published in 2013 by Verlag Zeitschrift für Naturforschung in cooperation with the Max Planck Society for the Advancement of Science under a Creative Commons Attribution-NoDerivs 3.0 Germany License.

On 01.01.2015 it is planned to change the License Conditions (the removal of the Creative Commons License condition "no derivative works"). This is to allow reuse in the area of future scientific usage.

$Y$  indicates the treatment temperature ( $T_{\text{treat}}$ ) and  $x$  the composition.

The X-ray diffraction (XRD) spectra were collected using a  $\theta$ - $2\theta$  conventional equipment (Siemens D500) with a  $\text{Mo-K}\alpha$  wavelength.

The Mössbauer absorption spectra were obtained in a standard transmission geometry, using a source of  $^{57}\text{Co}$  in rhodium (370 MBq). A calibration was performed using a 25  $\mu\text{m}$  thick natural  $\alpha$ -Fe foil; the isomer shift values are referred to  $\alpha$ -Fe. The measurements were carried out at room temperature on powder samples contained in a Plexiglas holder. The surface density of the absorbers has been chosen in order to optimize the time of measurement; this density ranges from 80 to 170  $\text{mg}/\text{cm}^2$  for the different samples. The Mössbauer absorption spectra have been examined by fitting the data by peaks with Lorentzian shape, using a least squares method. Actually, amorphous and nanocrystalline materials do not show simple Lorentzian line shapes, owing to structural disorder and to paramagnetic relaxation [13]; therefore this fitting procedure must be considered an approximation.

### 3. Results

#### XRD

The XRD spectra of samples treated at 700 and 900  $^{\circ}\text{C}$  are reported in Figure 1. In the spectrum of the  $\text{Fe}_{16.9}700$  sample two broadened bands emerge on the amorphous silica background, which are consistent with the  $d$  spacing typical of most iron hydroxides, oxyhydroxides or oxides. They indicate the presence of iron oxide (or hydroxide) nanoparticles, in agreement with previous TEM observations [1, 2], at the limits of observation of the XRD analysis (3 - 4 nm). In the spectrum of the  $\text{Fe}_{16.9}900$  sample two peaks appear which, also on the basis of the ferrimagnetic behavior of the material [1], can be ascribed to the presence of the  $\gamma$ - $\text{Fe}_2\text{O}_3$  phase. The spectra of the  $\text{Fe}_{9.1}$ ,  $\text{Fe}_{16.9}$  and  $\text{Fe}_{23.0}$  samples exhibit the same features. In the spectra of the  $\text{Fe}_{28.5}$  and  $\text{Fe}_{33.2}$  samples treated at 900  $^{\circ}\text{C}$  additional peaks appear (Figure 1). They could be attributable to the  $\alpha$ - $\text{Fe}_2\text{O}_3$  antiferromagnetic phase, which is the most thermally stable form observed at high  $T_{\text{treat}}$ ; but the alternative or simultaneous presence of the  $\varepsilon$ - $\text{Fe}_2\text{O}_3$  phase, also antiferromagnetic, cannot be excluded [14, 15]. The appearance of the new phases at  $T_{\text{treat}} = 900$   $^{\circ}\text{C}$

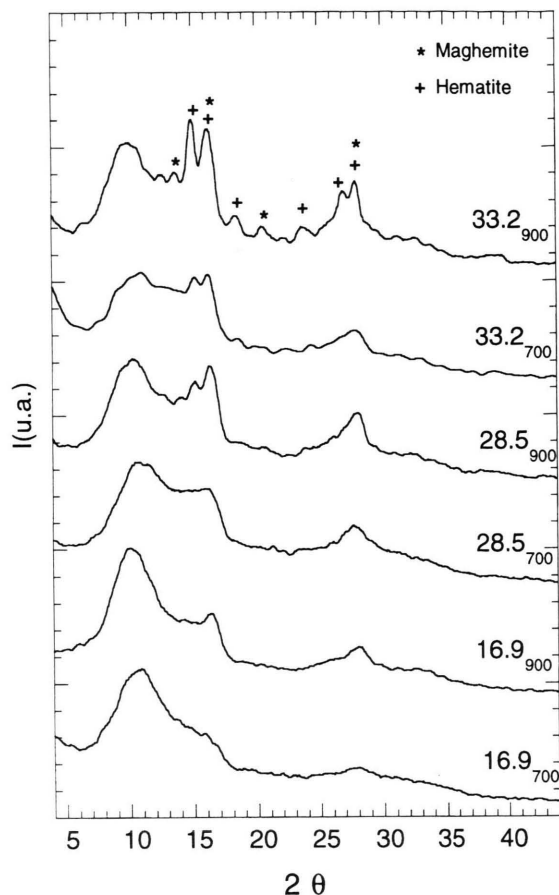


Fig. 1. XRD data of the samples treated at 700 and 900  $^{\circ}\text{C}$ .

is accompanied by a further growth of the  $\gamma$  phase. It seems therefore that the progressive  $\gamma$  to  $\alpha$  (and/or  $\varepsilon$ ) transformation is accompanied by simultaneous growth of the  $\gamma$  phase at the expense of the residual amorphous phase. In the spectrum of  $\text{Fe}_{33.2}700$  sample, faint peaks ascribable to  $\alpha$  (and/or  $\varepsilon$ ) phase are already present.

All the samples treated at  $T \leq 500$   $^{\circ}\text{C}$  are mostly amorphous [2].

#### Mössbauer spectroscopy

In Fig. 2 the Mössbauer absorption spectra of the samples at 9.1 and 33.2 wt% of  $\text{Fe}_2\text{O}_3$ , treated at 300  $^{\circ}\text{C}$ , are shown. In Table 1 the results of the least squares fits are given; the values of the isomer shift ( $\delta$ ), quadrupole splitting ( $\Delta$ ), full width at half maximum ( $\Gamma$ ), internal magnetic field ( $B$ ) and relative area of the components are reported.

Table 1. Mössbauer parameters as obtained by fitting the spectra of the indicated samples. The values of isomer shift ( $\delta$ ), quadrupole splitting ( $\Delta$ ), full width at half maximum of the peaks ( $\Gamma$ ), internal magnetic field ( $B$ ) and relative area of the peaks are given.

Sample	Component	$\delta$ mm/s	$\Delta$ mm/s	$\Gamma$ mm/s	$B$ T	Area %
Fe <sub>9.1</sub> 300	I	0.34	0.66	0.38		44
	II	0.34	1.13	0.51		56
Fe <sub>33.2</sub> 300	I	0.34	0.61	0.37		51
	II	0.33	1.06	0.45		49
Fe <sub>9.1</sub> 700	I	0.34	0.80	0.44		50
	II	0.33	1.41	0.56		50
Fe <sub>33.2</sub> 700	I	0.34	0.64	0.40		47
	II	0.34	1.16	0.54		49
	III	0.38	-0.12	0.33	52	4

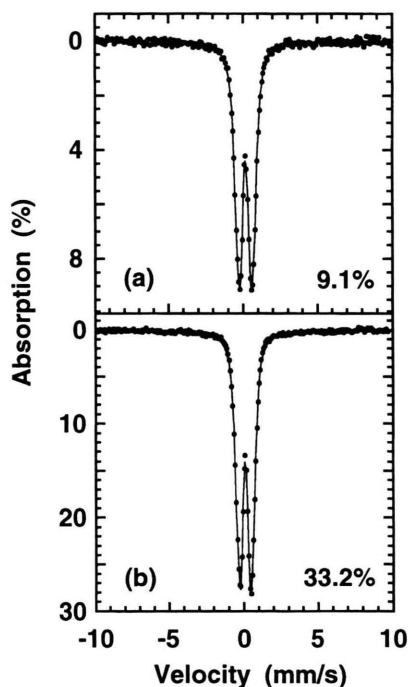


Fig. 2. Mössbauer spectra of the Fe<sub>9.1</sub> sample (a) and Fe<sub>33.2</sub> sample (b) treated at 300 °C. The experimental points (dots) and the fitted spectra (continuous line) are shown.

The spectra of these samples treated at 300 °C show the features of the spectra of paramagnetic materials. The experimental data can be well fitted by two quadrupole doublets, which result to have the same isomer shift (IS) but very different quadrupole splitting (QS). The values of isomer shift are typical of trivalent iron [16, 17]. The two components correspond to two different sites of the iron. Considering

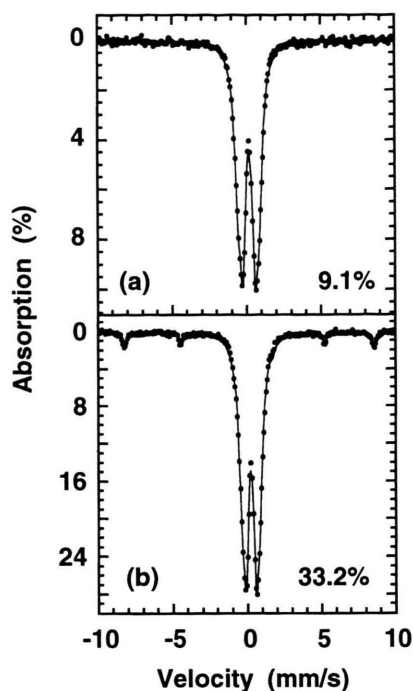


Fig. 3. Mössbauer spectra of the Fe<sub>9.1</sub> sample (a) and Fe<sub>33.2</sub> sample (b) treated at 700 °C. The experimental points (dots) and the fitted spectra (continuous line) are shown.

that the QS of the high spin Fe<sup>3+</sup> increases with the distortion of the iron site, the component I (smaller QS) corresponds to iron in less distorted sites, while the component II is due to atoms in more distorted sites [17]. In our previous work [1] we interpreted the two sites as superficial sites (more distorted) and internal sites (less distorted) of the nanoparticles. This interpretation is still valid since the observed ratio of about 50% indicates the presence of two structural sites of the amorphous ferric oxide also in the present situation. In fact, the slight differences in the sites percentages are consistent with the slight particle growth observed as a function of iron oxide concentration [2].

The absorption peaks of these samples are broadened with respect to a crystalline material, with full width at half maximum (FWHM) similar to that found for Fe<sup>3+</sup> in glasses; this broadening is comparable to that due to structural disorder [18, 19]. It agrees with the observation, made by TEM, that the ferric oxide is mainly amorphous.

Figure 3 shows the spectra of the samples at 9.1 wt% and 33.2 wt% treated at 700 °C; the parameters of the best fit are given in Table 1.

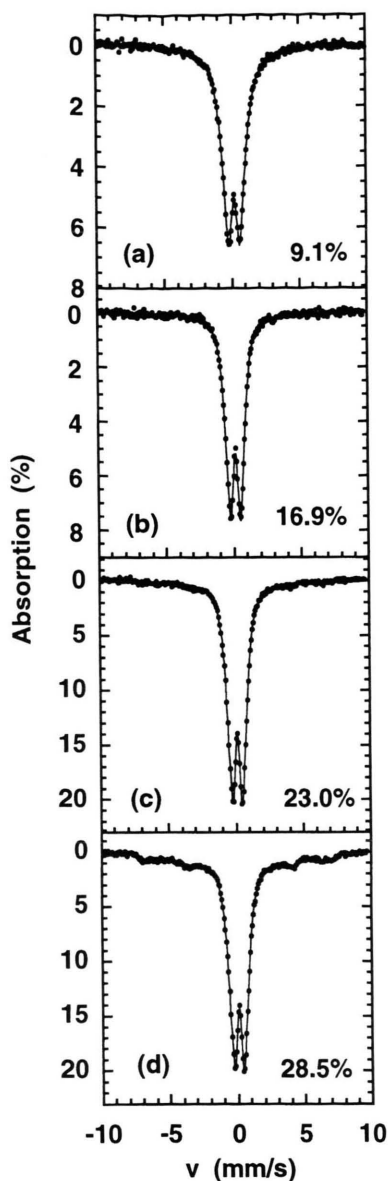


Fig. 4. Mössbauer spectra of the Fe<sub>9.1</sub> (a), Fe<sub>16.9</sub> (b), Fe<sub>23.0</sub> (c) and Fe<sub>28.5</sub> (d) samples treated at 900 °C. The experimental points (dots) and the fitted spectra (continuous line) are shown.

The spectrum of the Fe<sub>9.1</sub> sample treated at 700 °C shows the same features as the spectrum of the Fe<sub>9.1</sub>300 sample; the interpretation of the parameters is the same. The spectra of the samples from 16.9 to 28.5 wt% treated at 700 °C are similar to that of the Fe<sub>9.1</sub>700 sample. The spectrum of the Fe<sub>33.2</sub>700 sample shows the formation of a magnetically ordered phase; this phase corresponds to 4% of iron atoms.

Table 2. Mössbauer parameters as obtained by fitting the spectra of the indicated samples. The values of isomer shift ( $\delta$ ), quadrupole splitting ( $\Delta$ ), full width at half maximum of the peaks ( $\Gamma$ ) and internal magnetic field ( $B$ ) are given.

Sample	Component	$\delta$ mm/s	$\Delta$ mm/s	$\Gamma$ mm/s	$B$ T
Fe <sub>9.1</sub> 900	I	0.34	0.77	0.58	
	II	0.35	1.15	1.21	
Fe <sub>16.9</sub> 900	I	0.34	0.68	0.53	
	II	0.34	1.22	0.78	
Fe <sub>23.0</sub> 900	I	0.34	0.84	0.75	
	II	0.34	1.07	0.82	
Fe <sub>28.5</sub> 900	I	0.34	0.63	0.56	
	II	0.33	1.10	0.82	
	III	0.39		2.10	41
Fe <sub>33.2</sub> 900	I	0.33	0.82	0.72	
	II	0.37		0.34	52
	III	0.36		0.62	45
	IV	0.40		0.68	40
	V	0.27		0.98	27

The values of the parameters permit to identify this phase as  $\alpha$ -Fe<sub>2</sub>O<sub>3</sub>, in agreement with the XRD result (Figure 1).

In Fig. 4 the Mössbauer absorption spectra of the samples with different concentration of oxide, treated 900 °C, are shown; in Table 2 the results of the least squares fits are given.

The spectrum of the Fe<sub>9.1</sub> sample treated at 900 °C has quadrupole doublets with FWHM much larger than the samples treated at 700 °C. The FWHM of the component II ( $\Gamma = 1.21$  mm/s) cannot be due to structural disorder; it can be ascribed to phenomena related to paramagnetic relaxation [13]. The relaxation time depends on the magnetization of the material and is bigger in ferrimagnetic than in antiferromagnetic materials [11, 12, 20, 21]; on the other hand, in the superparamagnetic state the peak width increases with the relaxation time [13]. These measurements show that at temperatures between 700 °C and 900 °C there is the main transformation of the amorphous oxide into the ferrimagnetic oxide. The features of the spectrum indicates the formation of  $\gamma$ -Fe<sub>2</sub>O<sub>3</sub> [12].

Also in the samples with concentration from 16.9 to 28.5 wt%, the  $\gamma$ -Fe<sub>2</sub>O<sub>3</sub> appears in the spectra of the samples treated at 900 °C.

The spectra of the Fe<sub>16.9</sub>900 and Fe<sub>23.0</sub>900 samples can be fitted by two quadrupole doublets; the Mössbauer parameters are similar to those of the Fe<sub>9.1</sub>900 sample. It indicates that the samples are in a superparamagnetic state. At a concentration of Fe<sub>2</sub>O<sub>3</sub> of 28.5 wt%, a further structure appears in the



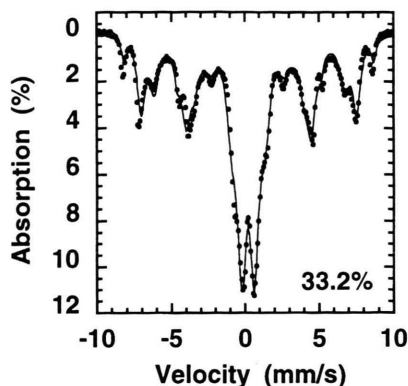


Fig. 5. Mössbauer spectrum of the Fe<sub>33.2</sub> sample treated at 900 °C. The experimental points (dots) and the fitted spectra (continuous line) are shown.

spectrum, which can be described by a magnetic sextuplet. This magnetic splitting with broad peaks is mainly due to the magnetic blocking of the biggest nanoparticles of  $\gamma$ -Fe<sub>2</sub>O<sub>3</sub> and corresponds to about 27% of iron atoms [12].

The spectrum of the Fe<sub>33.2</sub>900 sample is shown in Figure 5. This spectrum has been fitted by means of one quadrupole doublet and four magnetic sextuplets; the ratios of the peak amplitudes within each sextuplet have been fixed to 2/1.5/1. The quadrupole doublet points out the presence of superparamagnetic particles of  $\gamma$ -Fe<sub>2</sub>O<sub>3</sub>. The contribution with a magnetic field of 52 T is due to  $\alpha$ -Fe<sub>2</sub>O<sub>3</sub> formed in the sample [22]; this well-crystallized phase has already been formed in the Fe<sub>33.2</sub> sample treated at 700 °C. The magnetic sextuplet with field of 45 T is the sextuplet which gives the biggest contribution to the resonant absorption; it comes from the magnetic blocking of nanoparticles of  $\gamma$ -Fe<sub>2</sub>O<sub>3</sub> and corresponds to about 25% of iron atoms. This result is consistent with the isothermal magnetization curves previously reported [2], where the saturation value (about 20 emu/g) was found much lower than that of bulk  $\gamma$ -Fe<sub>2</sub>O<sub>3</sub> (82 emu/g at 4.2 K). The components with magnetic fields of 40 T (19%) and 27 T (17%) are probably due to the presence of other oxides; in particular a phase with a field of about 40 T at room temperature, identified as  $\epsilon$ -Fe<sub>2</sub>O<sub>3</sub>, has been already observed in similar nanocomposites [14, 15].

#### 4. Discussion and Conclusions

Fe<sub>2</sub>O<sub>3</sub>-SiO<sub>2</sub> composites were prepared within a wide range of compositions. Superparamagnetic be-

havior is exhibited by all the samples, indicating that the size of iron oxide grains is always in the nanometer range, even at the maximum iron content and/or after the highest thermal treatment. The increase of iron content gives rise to a small particle growth, while the spread of sizes around the average value increases in a more significant way [2]. The growth of the particles is also produced by the increase of treatment temperature of the samples [1]. The size range is between that of single domain particles (< 15 - 20 nm) and that of a superparamagnetic assembly of atoms ( $\sim$  1 nm).

Although the grain size grows slightly with heat treatment, the Mössbauer spectra show a very steep increase of the peak width at  $T_{\text{treat}} = 900$  °C, indicating the formation of the ferrimagnetic  $\gamma$ -Fe<sub>2</sub>O<sub>3</sub> phase, at all the explored compositions, from the antiferromagnetic amorphous Fe<sub>2</sub>O<sub>3</sub> phase. The experimental evidence is in favor of the main  $\gamma$ -Fe<sub>2</sub>O<sub>3</sub> formation only at  $T_{\text{treat}} = 900$  °C, while amorphous Fe<sub>2</sub>O<sub>3</sub> is the most abundant phase in samples treated at  $T_{\text{treat}}$  smaller or equal to 700 °C, as pointed out by TEM dark field micrographs and Mössbauer spectra.

The result indicates that the stability of the iron oxide phases is strongly affected by the supporting material (host matrix), since  $\gamma$ -Fe<sub>2</sub>O<sub>3</sub> is unstable in comparison with  $\alpha$ -Fe<sub>2</sub>O<sub>3</sub> at such high temperatures. Also, in the Fe<sub>33.2</sub> samples the  $\alpha$ -Fe<sub>2</sub>O<sub>3</sub>, observed by the Mössbauer spectra, is already formed at 700 °C and does not change in per cent at 900 °C. It supports a direct formation of the  $\alpha$ -Fe<sub>2</sub>O<sub>3</sub> from the amorphous phase.

The Fe<sub>28.5</sub> and Fe<sub>33.2</sub> samples treated at 900 °C also show a component of  $\gamma$ -Fe<sub>2</sub>O<sub>3</sub> in the blocked state at room temperature. On the other hand, the magnetic susceptibility measured by SQUID (superconducting quantum interference device) shows blocked particles below 110 K [2]. This is explained by the different time of measurement of the different techniques; the Mössbauer spectroscopy has a measurement time ( $\tau_m \sim 10^{-8}$  s) which is much shorter than the time of the SQUID ( $\tau_m \sim 100$  s). The observation of the blocking only in the more concentrated samples indicates a bigger size of the  $\gamma$ -Fe<sub>2</sub>O<sub>3</sub> nanoparticles with respect to the less concentrated ones.

The reported results point out that this method of preparation produces nanocomposites with about only  $\gamma$ -Fe<sub>2</sub>O<sub>3</sub> at concentration of Fe<sub>2</sub>O<sub>3</sub> up to 23 wt%. At higher concentration, the growth of the particles favors the formation of other oxide phases ( $\alpha$  and  $\epsilon$  phase) along with the  $\gamma$  phase.

### Acknowledgements

This work has been supported by CNR 95.01588 CT 11 grant and MURST (Rome, Italy).

- [1] G. Concas, G. Ennas, D. Gatteschi, A. Musinu, G. Piccaluga, C. Sangregorio, G. Spano, J. L. Stanger, and D. Zedda, *Chem. Mater.* **10**, 495 (1998).
- [2] C. Cannas, D. Gatteschi, A. Musinu, G. Piccaluga, and C. Sangregorio, *J. Phys. Chem. B* **102**, 7721 (1998).
- [3] M. N. Ashua, *J. Mater. Sci. Lett.* **12**, 1705 (1993).
- [4] D. Niznansky, J. L. Rehspringer, and M. Drillon, *IEEE Trans. on Magnetics* **30**, 821 (1994).
- [5] M. Guglielmi and G. Principi, *J. Non-Cryst. Solids* **48**, 161 (1982).
- [6] C. R. F. Lund and J. A. Dumesic, *J. Phys. Chem.* **85**, 3175 (1981).
- [7] J. M. D. Coey, *Phys. Rev. Letters* **27**, 1140 (1971).
- [8] K. Haneda and A. H. Morrish, *Solid State Commun.* **22**, 779 (1977).
- [9] P. Ayyub, M. Multani, M. Barma, V. R. Polkar, and R. Vijayaraghavan, *J. Phys. C: Solid State Phys.* **21**, 2229 (1988).
- [10] T. Ida, H. Tsuiki, A. Ueno, K. Tohji, K. Udagawa, K. Iwai, and H. Sano, *J. Catalysis* **106**, 428 (1987).
- [11] E. Tronc, *Nuovo Cim.* **18D**, 163 (1996).
- [12] E. Tronc, P. Prene, J. P. Jolivet, F. d'Orazio, F. Lucari, D. Fiorani, M. Godinho, R. Cherkaoui, M. Nogues, and J. L. Dormann, *Hyperfine Interactions* **95**, 129 (1995).
- [13] H. H. Wickman, in *Mössbauer Effect Methodology*, ed. by I. J. Gruverman, Plenum Press, New York 1966, Vol. 2, p. 39.
- [14] I. Dezsi and J. M. D. Coey, *Phys. Stat. Sol.* **15(a)**, 681 (1973).
- [15] C. Chanéac, E. Tronc, and J. P. Jolivet, *Nanostruct. Mater.* **6**, 715 (1995).
- [16] P. Gütlich, R. Link, and A. Trautwein, *Mössbauer Spectroscopy and Transition Metal Chemistry*, Springer-Verlag, Berlin 1978, p. 56.
- [17] M. Darby Dyar, *Amer. Mineral.* **70**, 304 (1985).
- [18] G. Concas, F. Congiu, C. Muntoni, and G. Pinna, *J. Phys. Chem. Solids* **56**, 887 (1995).
- [19] C. R. Kurkjian and E. A. Sigety, *Phys. Chem. Glasses* **9**, 73 (1968).
- [20] W. F. Brown Jr., *Phys. Rev.* **130**, 1677 (1963).
- [21] S. Mørup, H. Topsøe, and J. Lipka, *J. Phys.* **37**, C6-287 (1976).
- [22] E. Murad and J. H. Johnston, in *Mössbauer Spectroscopy Applied to Inorganic Chemistry*, ed. by G. J. Long, New York 1987, Vol.2, p. 507.